# Numerical homogenization of polymer/clay nanocomposites by the boundary element method

J. PTASZNY, P. FEDELIŃSKI

*Department of Strength of Materials and Computational Mechanics*
*Silesian University of Technology*
*ul. Konarskiego 18a*
*44-100 Gliwice, Poland*
*e-mails: Jacek.Ptaszny@polsl.pl, Piotr.Fedelinski@polsl.pl*

THE PAPER DEALS WITH THE NUMERICAL HOMOGENIZATION of polymer/clay nanocomposites by using the boundary element method (BEM). The reinforcement has the form of stacks of parallel clay sheets modelled by effective isotropic particles. Two-dimensional representative volume elements (RVEs), containing randomly distributed parallel rectangular particles, are modelled and five plane-strain elastic constants of the orthotropic composite are analysed: two Young's moduli, shear modulus and two Poisson's ratios. The results are compared to experimental data, finite element method (FEM) results, and analytical models as well. The positive-definiteness and symmetry of the apparent compliance matrix are verified. All the comparisons and tests confirm validity of the applied method.

**Key words:** boundary element method, effective particle, elastic constants, homogenization, nanocomposites.

## 1. Introduction

POLYMER/CLAY NANOCOMPOSITES are characterized by enhanced mechanical properties at low weight fractions of reinforcement in comparison to other types of composites. The reinforcement structure can be composed of exfoliated clay sheets or stacks of parallel nanoclay sheets. During the design of structures, homogenized properties of composite materials are required. The overall properties can be determined by applying analytical, empirical or numerical methods. The most popular ones are: Mori–Tanaka method (M-T), Halpin–Tsai method (H-T), self-consistent method, Hashin-Shtrikman bounds and the analysis of a representative volume element (RVE) by the finite element method (FEM). In recent years, many papers concerning the problem of the homogenization of nanocomposites has been published. A short chronological review of selected papers is given below.

WANG and PYRZ in [12] presented the theory and formulas for the prediction of overall moduli of layered silicate-reinforced polymeric nanocomposites. Formulas for the moduli of composite materials reinforced with transversely isotropic spheroids, were derived from the M-T method. The predictions were compared to approximate formulas found in the literature for isotropic thin oblate spheroids. In the second part of the cited work [13], the authors applied their formulas to the analysis of various montmorillonite silicate-reinforced polymeric nanocomposites. SHENG et al. [9] applied a multiscale modelling strategy, taking into account the hierarchical morphology of the polymer/clay nanocomposites, to the prediction of homogenized properties of the materials. The clay particles can have the form of exfoliated clay sheets, of nanometer level thickness or stacks of parallel clay sheets separated from one another by interlayer galleries of nanometer level height. It was shown that in the latter case the stacks could be represented by effective particles. The authors discussed in detail the issues related to the evaluation of properties of the clay sheets and the effective particles. Two-dimensional FEM simulations were performed involving isotropic effective particles and the effective longitudinal Young's modulus was determined. The results were verified by the comparison to experimental data, and the M-T and H-T models. HBAIEB et al. [6] analyzed 2-D (plane stress) and 3-D FEM models of the polymer/clay nanocomposites with aligned and randomly oriented particles. They calculated the effective Young's modulus in the axial direction, and Young's modulus of the isotropic effective medium, according to the analysed case. The results were compared to the M-T model. The authors concluded that the 2-D models were inappropriate to the analysis of the composites as the models did not predict accurately the stiffness of the composites. FIGIEL and BUCKLEY [3] calculated elastic constants for the layered-silicate/polymer nanocomposite with intercalated morphology by using the effective particle concept. Two methods were applied: plane strain FEM analysis and the M-T method. Young's moduli in two perpendicular directions and shear modulus were determined. It was shown that the effective particle concept was valid if full anisotropy of the effective particle was taken into account. For small volume fraction of effective particles, the results for both the cases of particles were close to each other. GÓRSKI and FEDELIŃSKI [4] modelled 2-D RVEs of the nanocomposites by using coupled boundary and finite element methods (BEM/FEM). The matrix was modelled by the BEM, and the reinforcement by beam finite elements. The authors considered both the aligned and randomly distributed particles. It was shown that the proposed method was more effective than the FEM, in terms of the number of degrees of freedom of the numerical model. In the recent paper by FEDELIŃSKI et al. [2], different formulations of the BEM were presented, for the analysis of composites containing rigid or deformable stiffeners and inclusions. The developed computer codes were used to compute effective elastic or piezoelectric material properties by the analysis

of 2-D RVEs or unit cells. One of the analysed materials was a polymer/clay nanocomposite reinforced with stacks of clay sheets.

In the present work, the polymer/clay nanocomposites reinforced by stacks of parallel clay sheets are analysed by the BEM. In the preliminary investigations the stacks are represented by isotropic effective particles. Two-dimensional RVEs of the composites are analysed in plane strain, by the formulation involving many identical inclusions. The 2-D plane strain model can give satisfactory results, as it can be found in the literature [3, 9]. Periodic boundary conditions are imposed. The determined effective elastic constants are: two Young's moduli, shear modulus and two Poisson's ratios. The numerical results are compared to other ones (analytical, semi-empirical, numerical and experimental) shown in the literature. The validity of the model is also verified by the positive-definiteness and symmetry tests of the effective compliance matrix of the material.

The novelty of the paper is the numerical homogenization of the nylon/clay nanocomposites by using the BEM, which is a new application of the method. The BEM can be effective in the numerical homogenization and thus competitive for the FEM, usually applied in this field. In the case of numerical homogenization, where no volume forces occur, only boundaries of the analysed RVE are discretized. The main advantages of the BEM are easy preparation of the numerical model and small amounts of data and results. The advantages are implied by the fact that the numerical homogenization requires only the knowledge of the RVE boundary quantities. As it has been shown in the literature preview, authors usually do not determine the full set of elastic constants. The constants calculated in this work fully define the overall elastic properties. The knowledge of the properties is crucial for the multi-scale modelling of elements made of inhomogeneous materials loaded arbitrarily.

The article is organized as follows: Section 2 contains the characterization of the analysed nanocomposites. In Section 3 the procedure of numerical homogenization is briefly described. Section 4 contains the description of the BEM, including the formulation for many identical inclusions. Section 5 includes the description of the performed numerical tests and their results. Section 6 contains the discussion of the results and conclusions.

## 2. Characterization of the nanocomposites

This section contains a brief characterization of nanocomposites with polymer matrix, reinforced by intercalated nanoclay. Only basic information allowing for the development of a 2-D model is given. The detailed description of the materials can be found in the paper by Sheng et al. [9].

The structure of the nanocomposite is shown in Fig. 1. The polymer matrix contains parallel stacks of clay sheets (Fig. 1a), which can be modelled by rectan-
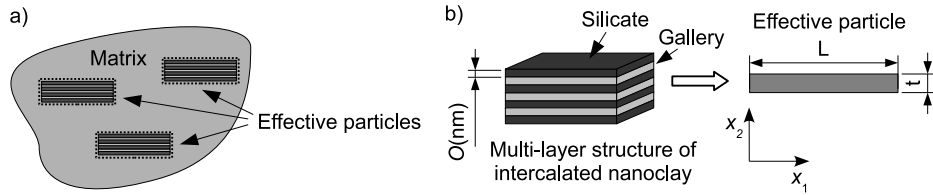
Fig. 1. Structure of the nanocomposite: a) matrix containing parallel effective particles, b) a stack of clay sheets modelled by the effective particle [9].

gular effective particles (Fig. 1b). The stacks consist of silicate layers separated by interlayer galleries. Both the constituents have thickness of few nanometers. The galleries are composed of surfactants and polymer matrix chains, that have penetrated the inter-silicate layers during various stages of manufacturing. A typical number of silicate layers is 2 to 4. The layers are comprised of repetitive, atomic lattice cells. Parameters of the layers, such as particle aspect ratio, volume fraction of the particle (in terms of clay weight fraction), and particle stiffness can be obtained from the molecular dynamics simulation. If the parameters of the clay sheets and galleries are known, the stacks can be modelled by effective particles. It is assumed that the effective particles are equivalent to the stacks in terms of the aspect ratio $L/t$ (where $L$ is length of the particle/stack and $t$ is its thickness), weight fraction $f_p$ and finally, overall mechanical properties. It should be mentioned that the determination of effective properties of the nanocomposite reinforcement is a very demanding task and requires the usage of advanced methods. There are many issues involved, which are not related directly to the problem considered in this article, and thus they are not discussed.

According to the literature, different models of the reinforcement can be applied, on different levels of simplification (Fig. 2). When the stack is considered as laminate (Fig. 2a), elastic constants for the effective particle can be calculated by continuum analytical models. The particle can be then considered as homogeneous and anisotropic (Fig. 2b), or isotropic (Fig. 2c) to make further homogenization process simpler. The particle constants, together with their geometry and properites of the polymer matrix, can be applied to the determination of homogenized properties of the composite. In this work, the simplest model, i.e. the isotropic effective particle is applied. The elastic constants are taken from the paper [9]. They will be presented in the section containing numerical tests.
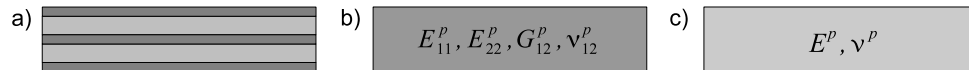


Fig. 2. Reinforcement models: a) stack of sillicate sheets, b) anisotropic effective particle, c) isotropic effective particle.

In order to determine the homogenized properties of the nanocomposite, the numerical analysis of RVEs by using the BEM is performed. The applied methods will be described in the next two sections.

## 3. Numerical homogenization

There are several groups of analytical methods of homogenization, namely: the rule of mixtures, effective medium approximation methods and asymptotic mathematical homogenization [7]. According to the literature review, the most popular analytical methods applied to the homogenization of the nanocomposites are the Mori–Tanaka (M-T) and Halpin–Tsai (H-T) methods. In fact, the H-T method is based on analytical formulas with empirically determined coefficients and can be called semi-empirical. In this article the model is treated as analytical for simplicity.

The analytical models do not always agree with experimental data. Furthermore, usually they do not provide the full set of elastic constants. Another method of homogenization is the numerical analysis of RVE. In the present work, the approach by Kouznetsova *et al.* [7] is applied. An RVE with periodic boundary conditions is considered. Figure 3 shows a deformed RVE with external boundary $\Gamma_0$ consisting of four parts: $\Gamma_B$, $\Gamma_L$, $\Gamma_T$ and $\Gamma_R$. The RVE shape is determined by the displacements of nodes (2) and (4), which are equal to:

$$(3.1) \quad u_i^{(2)} = \bar{\varepsilon}_{ij}(x_j^{(2)} - x_j^{(1)}), \quad u_i^{(4)} = \bar{\varepsilon}_{ij}(x_j^{(4)} - x_j^{(1)}), \quad i = 1, 2, \quad j = 1, 2,$$

where $\bar{\varepsilon}_{ij}$ denotes known components of macro-strain. The remaining points of the external boundary, including node (3), are tied to the nodes (2) and (4) by the following constraints:

$$(3.2) \quad u_i^{(R)} = u_i^{(L)} + u_i^{(2)} - u_i^{(1)}, \quad u_i^{(T)} = u_i^{(B)} + u_i^{(4)} - u_i^{(1)}, \quad i = 1, 2.$$
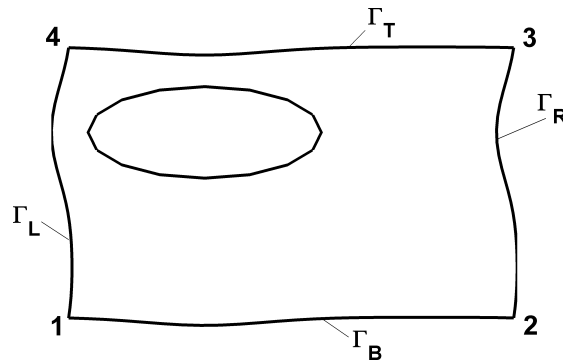


Fig. 3. A representative volume element deformed according to periodic boundary conditions.

It is also assumed that in respective points located on the mutually opposite parts of the boundary, traction forces are also opposite:

$$(3.3) \qquad t_i^B = -t_i^T, \qquad t_i^L = -t_i^R, \qquad i = 1, 2.$$

In order to satisfy all the conditions, respective constraints are introduced to the system of equation built by the applied numerical method (in this case the BEM).

The homogenized elastic moduli of a 2-D inhomogeneous material can be determined by performing three independent tests, namely: extension along two directions and shear (Fig. 4). All components of the averaged (macro-) strain tensor $\bar{\varepsilon}_{ij}$ $(i, j = 1, 2)$ can be calculated by using the following expression:

$$(3.4) \qquad \bar{\varepsilon}_{ij} = \frac{1}{L_1 L_2} \int_{\Gamma_0} \frac{1}{2}(u_i n_j + u_j n_i) \, d\Gamma_0,$$

where $L_1$ and $L_2$ denote the dimensions of RVE, and $n_j$ are components of the unit vector normal to the external boundary. In the three cases presented in the Figures 4a–4c, the selected strain components can be determined in a more simple way:

- for test 1 ($\delta_1$ is given):

$$(3.5) \qquad \bar{\varepsilon}_{11} = \frac{\delta_1}{L_1}, \qquad \bar{\varepsilon}_{22} = -\frac{\delta_2}{L_2};$$

- for test 2 ($\delta_2$ is given):

$$(3.6) \qquad \bar{\varepsilon}_{11} = -\frac{\delta_1}{L_1}, \qquad \bar{\varepsilon}_{22} = \frac{\delta_2}{L_2};$$

- and test 3 ($\delta_1$ is given):

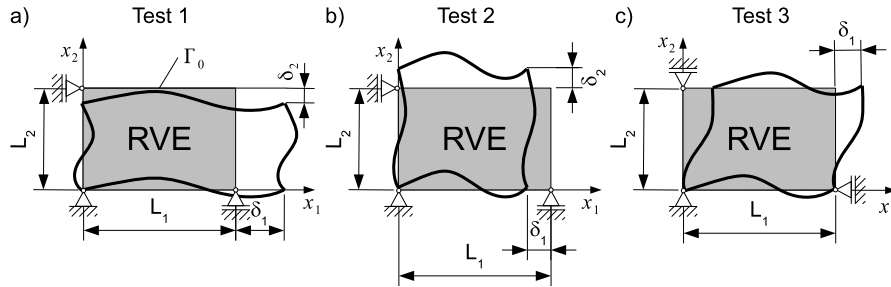$$(3.7) \qquad \bar{\varepsilon}_{12} = \frac{\delta_1}{2L_2}.$$



FIG. 4. Three tests by using RVE with periodic boundary conditions: a) extension along the $x_1$-axis, b) extension along the $x_2$-axis, c) shear.

The averaged stress components are calculated by using the equation:

$$(3.8) \qquad \bar{\sigma}_{ij} = \frac{1}{L_1 L_2} \int_{\Gamma_0} t_i x_j \, d\Gamma_0,$$

where $t_i$ denotes components of traction forces and $x_i$ are coordinates of a point located on $\Gamma_0$.

Assuming that the analysed 2-D material is linear-elastic and macroscopically orthotropic, the constitutive law can be written in the following way:

$$(3.9) \qquad \begin{pmatrix} \bar{\varepsilon}_{11} \\ \bar{\varepsilon}_{22} \\ 2\bar{\varepsilon}_{12} \end{pmatrix} = \begin{bmatrix} 1/E_{11} & -\nu_{21}/E_{22} & 0 \\ -\nu_{12}/E_{11} & 1/E_{22} & 0 \\ 0 & 0 & 1/G_{12} \end{bmatrix} \begin{pmatrix} \bar{\sigma}_{11} \\ \bar{\sigma}_{22} \\ \bar{\sigma}_{12} \end{pmatrix},$$

where the square matrix is the compliance of the material. It can be denoted by $S_{ij}$ $(i, j = 1, 2, 3)$. It depends on the engineering constants: Young's moduli: $E_{11}$ and $E_{22}$, shear modulus $G_{12}$ and Poisson's ratios: $\nu_{12}$ and $\nu_{21}$. By energetic considerations it can be deduced that the matrix $S_{ij}$ is symmetric and positively definite. The symmetry condition can be applied to the calculation of one of Poisson's ratios, assuming that the another one is known. Such situation is encountered in the application of analytical methods, which provide formulas for only one Poisson's ratio. In the case of numerical analysis, the symmetry condition can be employed in order to verify the validity of the numerical model.

By performing the three tests shown in the Figs. 4a–4c, one can define and solve a linear system of nine equations, with $S_{ij}$ as unknowns. Assuming that the material is orthotropic in macroscale, which means that respective elements of the compliance matrix are equal to zero, five engineering constants of the material can be calculated by using the following formulas:

$$(3.10) \quad E_{11} = \frac{1}{S_{11}}, \quad E_{22} = \frac{1}{S_{22}}, \quad G_{12} = \frac{1}{S_{33}}, \quad \nu_{12} = -\frac{S_{21}}{S_{11}}, \quad \nu_{21} = -\frac{S_{12}}{S_{22}}.$$

By using the above framework and a numerical method, the full set of homogenized elastic constants of a 2-D inhomogeneous material can be calculated. For the detailed description of the theory of numerical homogenization, please refer to the available literature (e.g. [7, 15], and others).

## 4. BEM modelling of composites

Consider a body: the matrix or the inclusion, which has the boundary $\Gamma$ and the domain $\Omega$. The body is homogeneous, isotropic and linear-elastic. It

is loaded by the boundary tractions $t_j$. The relation between the loading and displacements $u_j$ is expressed by the boundary integral equation [1]:

$$(4.1) \qquad c_{ij}(x')u_j(x') + \int_\Gamma T_{ij}(x,x')u_j(x')\,d\Gamma = \int_\Gamma U_{ij}(x,x')t_j(x')\,d\Gamma,$$

where $x'$ is a collocation point, $x$ is a boundary point, $c_{ij}$ is a constant which depends on the position of the point $x'$, $U_{ij}$ and $T_{ij}$ are fundamental solutions of elastostatics. The summation convention is used in the equation.

The external and internal boundaries of the matrix are divided into boundary elements. The elements with boundary nodes are shown in Fig. 5 (the elements are not drawn for the internal boundaries to make the figure readable). Displacements and tractions within each boundary element are interpolated by using nodal values and shape functions. The boundary integral equations (4.1) are used for nodes along external and internal boundaries of the body. As a result, a system of linear algebraic equations is built and solved for unknown displacements and tractions on respective parts of the boundary. It should be noticed that the computational complexity of the BEM is at least quadratic.
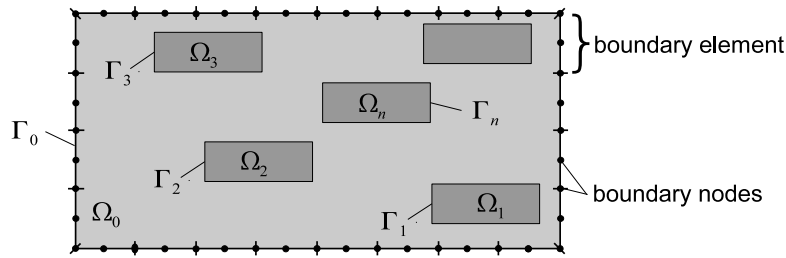


Fig. 5. Matrix with particles modelled by the BEM.

For the purpose of BEM modelling of composites, the formulation proposed by Yao *et al.* [14] can be applied. The domain of the whole structure is denoted by $\Omega_0$, and its boundary by $\Gamma_0$ (Fig. 5). There are $n$ particles with domains $\Omega_k$ and boundaries $\Gamma_k$ ($k = 1, 2, \ldots, n$). The following assumptions are made:
- the matrix contains identical particles; the particle shape is arbitrary;
- perfect bonding is assumed between the matrix and the inclusions, i.e. the conditions of continuity of displacements and equilibrium of tractions on the interfaces $\Gamma_k$ are satisfied;
- all the particles are located inside the matrix, i.e. the particles do not cross the external boundary $\Gamma_0$.

In the formulation, a system of equations is built for the matrix, and modified by using small matrix calculated for a single particle. Unknowns are only the quantities on the external boundary and displacements on the interfaces. The tractions on the interfaces are eliminated from the system of equations. Thus, a system with the reduced size is obtained as a result. The interface tractions can be calculated if necessary, by using the solution of the system.

In this work, a BEM code developed by the authors is applied. Quadratic boundary elements are used. The regular boundary integrals are calculated numerically by using 10-point Gauss quadrature, while the singular ones are calculated by a special logarithmic quadrature and the method of rigid body motion [1]. RVEs of composite materials are modelled by using the formulation for matrix with many particles described above. The periodic boundary conditions are applied by the modifications of the BEM system of equations and homogenized properties are calculated by the method shown in the previous section.

## 5. Numerical examples

Homogenized elastic constants of polymer/clay nanocomposite reinforced by intercalated particles are analyzed. The effective particles are modelled as rectangular inclusions. The RVEs are rectangles containing 60 identical inclusions, in plane strain. The materials of both the matrix and inclusions are linear elastic and isotropic. The periodic boundary conditions are imposed, with given displacements of respective corners of the RVE. Three tests were performed in order to calculate all the homogenized constants. The constants are: Young's moduli in two directions $E_{11}$ and $E_{22}$, shear modulus $G_{12}$ and two Poisson's ratios: $\nu_{12}$ and $\nu_{21}$. The results are compared to the M-T model for spheroidal penny-shape inclusions [9, 10], and H-T model for fibers with rectangular cross-sections [5].

Parameters of the analysed composite are [9]: length of the effective particles $L = 200$ nm, aspect ratio of the particles $L/t = 23$, with thickness $t$, Young's modulus of matrix $E_m = 4$ GPa, ratio of Young's modulus of particles to the modulus of matrix $E_p/E_m = 21$, Poisson's ratios of matrix and particles $\nu_m = 0.35$, $\nu_p = 0.28$, and the relation between the volume fraction of particles $f_p$ and the weight fraction $W_c$, $f_p/W_c = 1.2$. All the elastic constants are given for the plane strain case. The ratio of vertical to horizontal side length of the RVE is $1/2$. Six values of weight fraction are considered: $W_c = 1$–6% with 1% step. Geometry of a typical RVE with $W_c = 6\%$ is shown in Fig. 6.

The dimensions of the RVEs are adjusted to the weight (volume) fraction. To make the procedure of generation of random geometry efficient, it was assumed that the particles are uniformly distributed in the vertical direction, and only the location in the horizontal direction is randomly selected. Ten different models

FIG. 6. Geometry of a typical RVE.

are generated for each value of the reinforcement weight fraction. The numerical homogenization is performed by means of the techniques described in the previous sections. A full set of homogenized plane strain elastic constants of the nanocomposite, as a function of the reinforcement weigth fraction, is obtained as the result.

The boundaries of the models are discretized by 1 512 quadratic boundary elements. Each inclusion is discretized by 22 boundary elements. The number of degrees of freedom of each structure is equal to 6 048. As it can be seen in the Fig. 6, a particle can be located closely to the external boundary of the RVE or to other particles. Furthermore, the longer sides of the particle are near to each other due to the relatively large aspect ratio. This can affect the accuracy of the numerical integration of the singular fundamental solutions, and the boundary value problem solution - boundary displacements, tractions, and stresses calculated by means of the former quantities. The accuracy of calculated homogenized moduli is checked by the analysis of a single homogeneous RVE, containing inclusions made of the same material as the matrix, with the largest considered value of particle weight fraction (6%). The absolute relative error of the calculated homogenized Young's moduli is less than 0.4%, of the shear modulus less than 0.07%, and of Poisson's ratios less than 2%. It is assumed that the discretization provides sufficient accuracy of the calculated homogenized moduli.

The calculated values of respective moduli, compared to other models, are shown in the Figs. 7–10. All the homogenized properties are normalized in relation to respective moduli of the matrix. The obtained results are discussed below.

The BEM results of the Young's modulus $E_{11}$ agree very well with the experimental data provided by SHENG et al. [9] (Fig. 7). The BEM regression line is located between the experimental data points. The FEM model by SHENG et al. [9] slightly overestimate the modulus. Finally, M-T and H-T models overes-
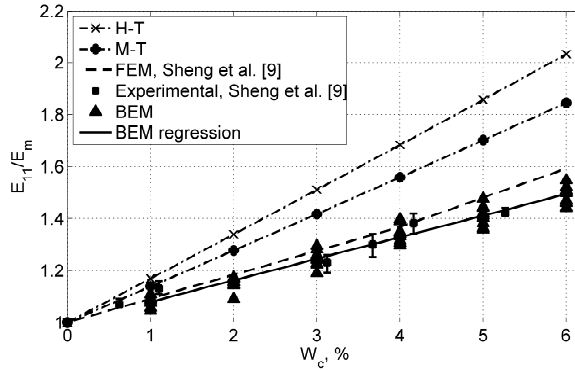
Fig. 7. Normalized homogenized Young's modulus $E_{11}$.

timate the modulus significantly. For 6% weight fraction, the relative difference between the M-T and BEM results exceeds 20%. Respective difference for the H-T model is over 30%. It can be seen that the BEM results are dependent on the randomly generated geometry, since there are variations of $E_{11}$ for each value of reinforcement weight fraction. These variations could be possibly eliminated by the analysis of RVEs containing a greater number of inclusions.

Most of the calculated values of the homogenized Young's modulus $E_{22}$ are between the values determined by the M-T and H-T models (Fig. 8). The H-T model underestimates the modulus, and for the largest value of $W_c$ the relative difference between the BEM regression and the H-T values is about 5%. The M-T model overestimates the modulus, with respective relative difference exceeding 10%. Similarly to the $E_{11}$ case, there are some variations of the calculated homogenized modulus for each value of $W_c$.
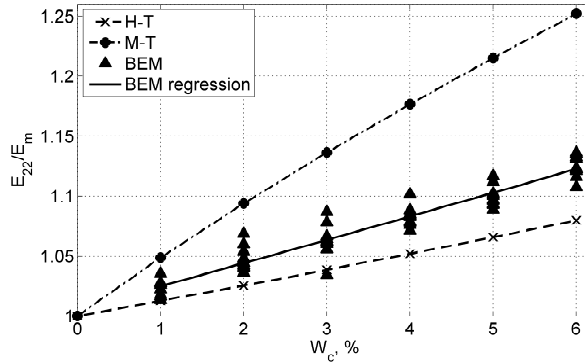


Fig. 8. Normalized homogenized Young's modulus $E_{22}$.

In the case of homogenized shear modulus $G_{12}$, the BEM results are also between the M-T and H-T values, however in this case, they are generally closer to the M-T model, since the relative difference for the largest value of $W_c$ is less than 1% (Fig. 9). Respective H-T value is greater than the BEM results by approximately 3%. It can be seen that in this case, the BEM results are insensitive to the RVE geometry changes, as opposed to the cases of moduli $E_{11}$ and $E_{22}$.
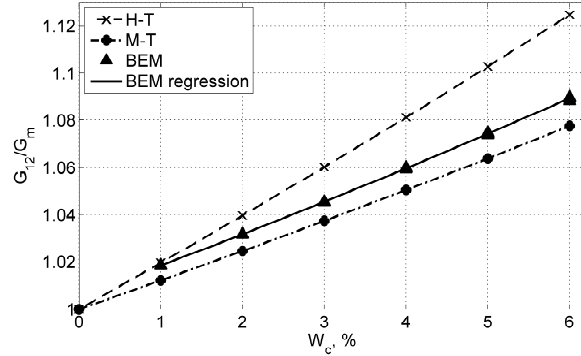


Fig. 9. Normalized homogenized shear modulus $G_{12}$.

The BEM results of homogenized Poisson's ratio $\nu_{21}$ are considered. The results are also compared to the M-T model, and the H-T one, consistent in this case with the rule of mixtures (ROM) (Fig. 10). It can be seen that the ratio is strongly sensitive to the RVE geometry changes, since the variations of $\nu_{21}$ are significant. Some of the BEM results exceed the range determined by the analytical models. The regression line is close to the M-T one and has a similar shape, but is moved downwards by a constant term, approximately equal to 0.02. The H-T/ROM results in this case are almost independent of $W_c$.
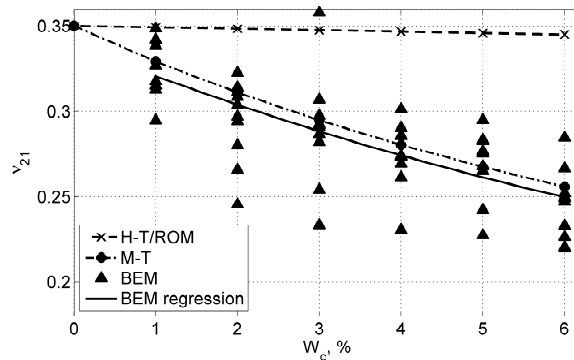


Fig. 10. Normalized homogenized Poisson's ratio $\nu_{21}$.

The values of $\nu_{12}$ obtained by the BEM (Fig. 11) are calculated by means of the elements of the effective compliance matrix. The corresponding homogenized Poisson's ratio predicted by the M-T and H-T models was calculated by using the compliance matrix symmetry condition:

$$(5.1) \qquad \nu_{12} = \frac{E_{11}}{E_{22}}\nu_{21},$$

and the previously calculated values of $\nu_{21}$, $E_{11}$ and $E_{22}$. Once again, some of the BEM results exceed the range determined by the analytical models. However, the regression line does not. Thus the qualitative dependence of results on $W_c$ is predicted correctly.
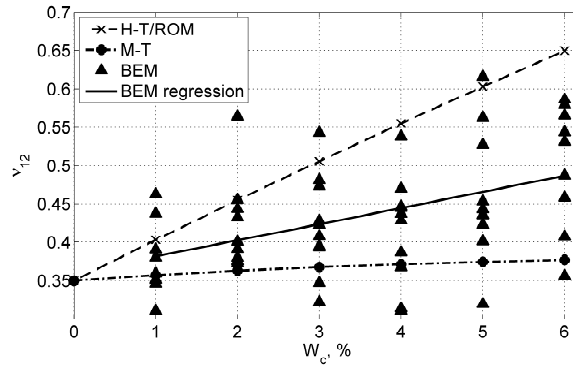


FIG. 11.  Normalized homogenized Poisson's ratio $\nu_{12}$.

All the elements of the compliance matrix that should be equal to zero, were also calculated. Mean value of all the elements calculated in all the tests, is equal to $10^{-8}$ MPa$^{-1}$. Furthermore for all the tests, absolute values of the considered quantities are by four orders of magnitude less than the Frobenius norm of the corresponding matrices. It can be assumed that the elements are small enough to be treated as zero. These results confirm that the material can be considered as macroscopically orthotropic.

The positive definiteness and symmetry of the compliance matrix state bounds for the homogenized elastic moduli. In order to verify the validity of the numerical model, apart from the comparison to analytical models, also the positive definiteness and symmetry tests are performed for each set of calculated homogenized moduli. All the compliance matrices built by using the moduli, satisfy the positive definiteness condition, as all their eigenvalues are positive. In the case of symmetry test, the following symmetry error is calculated:

$$(5.2) \qquad \Delta = \frac{\|S_{ij} - \bar{S}_{ij}\|}{\|\bar{S}_{ij}\|} \cdot 100\%,$$

where $\| \cdot \|$ denotes the Frobenius norm of a matrix, and $\bar{S}_{ij}$ is the symmetrized matrix:

$$(5.3) \qquad \bar{S}_{ij} = \frac{1}{2}\left(S_{ij} + S_{ji}\right).$$

The error is computed individually for each of the tests. The error is less than 5.5% and is not correlated with the reinforcement volume fraction $W_c$.

## 6. Conclusions

In this work, the polymer/clay nanocomposites, reinforced by stacks of parallel clay sheets, were analysed by the BEM and by the isotropic effective particle concept [9]. A special formulation for plates containing many identical inclusions was applied [14]. Two-dimensional RVEs containing randomly distributed parallel particles were analysed. Periodic boundary conditions were imposed. Five elastic moduli of the composite were calculated: Young's moduli in two perpendicular directions, shear modulus and two Poisson's ratios. Dependence of the moduli on the weight fraction of the reinforcement was investigted. The numerical results were compared to the analytical Mori–Tanaka and Halpin–Tsai models, numerical results obtained by the FEM, and experimental results [9]. The comparison confirmed the applicability of the proposed method to the solution of the homogenization problem.

It appeared that the results of homogenized Young's moduli and Poisson's ratios were sensitive to the particle distribution changes, as variations of the results were observed for a fixed value of reinforcement weight fraction. In the case of Young's moduli, the variation magnitude was similar to the range from tensile test for the Young modulus $E_{11}$, presented in the literature. In the case of Poisson's ratios the variations had much greater magnitudes, as some of the results exceeded the range determined by the M-T and H-T models. The variations could be caused by the moderate size of the RVEs, containing 60 particles. The variations could be possibly minimized by modelling of structures with a greater number of particles. In the case of shear modulus, very small variations of the results were observed for a given value of the reinforcement weight fraction.

In all the cases of elastic moduli, the BEM regression lines correctly predicted the qualitative dependences of the moduli on the weight fraction. The validity of the BEM model was also confirmed by the positive-definiteness test of all homogenized compliance matrices, and the symmetry error of the matrices in the range 0 to 5.5%, which are acceptable values. It is worth noticing that the symmetry error could be also caused by the moderate RVE size.

The developed model can be improved by modelling of RVEs with periodic geometry, i.e. containing inclusions intersecting the outer boundary. It is known

that such models can have a higher stiffness due to more intense interactions between the particles. The nanocomposites with greater values of the reinforcement weight (volume) fraction can be modelled by using anisotropic effective particles. This can be achieved by the BEM formulation involving the Stroh formalism [11]. Comparison between the effective moduli for the cases of isotropic and orthotropic effective particles would be interesting. Another important issues would be: the analysis of RVEs containing randomly oriented effective particles, and the development of 3-D BEM model of the nanocomposites.

It has been mentioned that the analysis of RVEs containing larger number of particles would reduce the variations of computed homogenized moduli. This can be a demanding task for the original collocation BEM due to its computational complexity, which is at least quadratic. To overcome this difficulty, one can consider an application of the fast multipole BEM. The complexity of the method (or a single iteration of the solution process to be exact) is linear. This relatively new version of the BEM was succesfully applied by Liu *et al.* [8] to the analysis of 3-D RVEs of another nanocomposites, reinforced with carbon-nanotubes, containing thousands of particles.

## Acknowledgements

## References

1. C.A. Brebbia, J. Dominguez, *Boundary elements an introductory course*, McGraw-Hill, New York 1992.

2. P. Fedeliński, R. Górski, G. Dziatkiewicz, J. Ptaszny, *Computer modelling and analysis of effective properties of composites*, Computer Methods in Materials Science, **11**, 3–8, 2011.

3. Ł. Figiel, C.P. Buckley, *Elastic constants for an intercalated layered-silicate/polymer nanocomposite using the effective particle concept. A parametric study using numerical and analytical continuum approaches*, Computational Materials Science, **44**, 1332–1343, 2009.

4. R. Górski, P. Fedeliński, *Evaluation of effective properties of nanocomposites by the coupled BEM/FEM*, Conference on Computational Modelling and Advanced Simulations CMAS 2009, J. Murín, V. Kutiš, R. Ďuriš [Eds], Book of abstracts, Bratislava, Slovak Republic, 47–48, 2009.

5. J.C. Halpin, J.L. Kardos, *Halpin-Tsai equations: A review*, Polymer Engineering and Science, **16**, 344–352, 1976.

6. K. Hbaieb, Q.X. Wang, Y.H.J. Chia, B. Cotterell, *Modelling stiffness of polymer/clay nanocomposites*, Polymer, **48**, 901–909, 2007.

7. V. Kouznetsova, W.A.M. Brekelmans, F.P.T. Baaijens, *An approach to micro-macro modeling of heterogeneous materials*, Computational Mechanics, **27**, 37–48, 2001.

8. Y. Liu, N. Nishimura, Y. Otani, *Large-scale modeling of carbon-nanotube composites by a fast multipole boundary element method*, Computational Materials Science, **34**, 173–187, 2005.

9. N. Sheng, M.C. Boyce, D.M. Parks, G.C. Rutledge, J.I. Abes, R.E. Cohen, *Multiscale micromechanical modeling of polymer/clay nanocomposites and the effective clay particle*, Polymer, **45**, 487–506, 2004.

10. G.P. Tandon, G.J. Weng, *The effect of aspect ratio of inclusions on the elastic properties of unidirectionally aligned composites*, Polymer Composites, **5**, 327–333, 1984.

11. T.C.T. Ting, *Anisotropic elasticity. Theory and applications*, Oxford University Press, New York–Oxford 1996.

12. J. Wang, R. Pyrz, *Prediction of the overall moduli of layered silicate-reinforced nanocomposites, part I: basic theory and formulas*, Composites Science and Technology, **64**, 925–934, 2004.

13. J. Wang, R. Pyrz, *Prediction of the overall moduli of layered silicate-reinforced nanocomposites, part II: analyses*, Composites Science and Technology, **64**, 935–944, 2004.

14. Z. Yao, F. Kong, X. Zheng, *Simulation of 2D elastic bodies with randomly distributed circular inclusions using the BEM*, Electronic Journal of Boundary Elements, **1**, 270–282, 2003.

15. T.I. Zohdi, P. Wriggers, *An Introduction to Computational Micromechanics*, Springer-Verlag, Berlin, Heidelberg 2008.